# Moderate-pressure Synthesis and Neutron Diffraction Study of New Metastable Oxides

Jose Antonio Alonso[a], Javier Sánchez-Benítez[b], Horacio Falcón[a], Maria Jesus Martínez-Lope[a], and Angel Muñoz[c]

[a] Instituto de Ciencia de Materiales de Madrid, CSIC, Cantoblanco, E-28049 Madrid, Spain
[b] Centre for Science at Extreme Conditions and School of Engineering and Electronics, University of Edinburgh, King's Buildings, Mayfield Road, Edinburgh EH9 3JZ, UK
[c] Dpto. de Física Aplicada, EPS, Universidad Carlos III, Avda. Universidad 30, E-28911, Leganés-Madrid, Spain

Reprint requests to Prof. Dr. J. A. Alonso. E-mail: ja.alonso@icmm.csic.es

Z. Naturforsch. **61b,** 1507 – 1514 (2006); received July 6, 2006

We have synthesized two new series of metastable oxides, namely $RE\mathrm{Mn_2O_5}$ and $RE\mathrm{Cu_3Mn_4O_{12}}$ ($RE$ = rare earths) under moderate pressure conditions. A novel series of ferrimagnetic oxides has been obtained by replacing $Mn^{3+}$ by $Fe^{3+}$ in the parent $RE\mathrm{Mn_2O_5}$ compounds ($RE$ = Y, Dy, Ho, Er, Tm, Yb). The crystal structure has been studied by neutron powder diffraction (NPD); it contains chains of edge-linked $Mn^{4+}O_6$ octahedra connected *via* dimeric groups of $Fe^{3+}O_5$ square pyramids. The magnetic susceptibility and the thermal evolution of the NPD patterns reveal the onset of a ferrimagnetic structure below $T_C \approx 165$ K, characterized by the propagation vector $k = 0$. Immediately below $T_C$, the $Fe^{3+}$ and $Mn^{4+}$ moments lie in an antiparallel arrangement along the $c$-axis direction. At lower temperatures, the magnetic moment of the rare-earth cations also participates in the magnetic structure, adopting a parallel arrangement with the $Fe^{3+}$ spins.

Some new derivatives of $\mathrm{CaCu_3Mn_4O_{12}}$ have been prepared at moderate pressures of 2 GPa by replacing $Ca^{2+}$ by $RE^{3+}$ cations in the series $RE\mathrm{Cu_3Mn_4O_{12}}$ ($RE$ = Pr, Sm, Eu, Gd, Tb, Dy, Ho, Tm, Yb); the concomitant electronic injection leads to a substantial contribution to $T_C$. The crystal structures of the new materials were refined in the space group $Im\bar{3}$ from NPD data for the non-absorbing $RE$ cations. The unit cell parameters are considerably expanded with respect to $\mathrm{CaCu_3Mn_4O_{12}}$, as a result of the electronic injection. The r. t. magnetic structure displays a ferrimagnetic coupling between $Mn^{3+/4+}$ and $Cu^{2+}$ spins; at low temperatures there is an antiferromagnetic coupling of the $RE^{3+}$ moments with the Mn substructure, which substantially reduces the susceptibility and the saturation magnetization.

*Key words:* Perovskite Oxide, Colossal Magnetoresistance, Ferrimagnetic Oxide, Neutron Powder Diffraction, Unusual Oxidation States

## Introduction

Many appealing properties such as high-temperature superconductivity, metallic behaviour and metal-insulator transitions or colossal magnetoresistance are often observed in complex oxides containing transition metals in intermediate or unusual oxidation states such as $Mn^{4+}$, $Cr^{4+}$, $Ni^{3+}$, $Cu^{3+}$ *etc.* In many cases these oxides are metastable and must be stabilized under special synthetic conditions, such as soft chemistry procedures or high-pressure chemistry. In particular, high-pressure chemistry is a powerful tool for the preparation of metastable oxides. High-pressure synthesis has been invaluable in the stabilization of paradigmatic oxides with singular properties. Some examples are the $\mathrm{HgBa_2Ca_2Cu_3O_8}$ cuprate [1], exhibiting a record superconducting critical temperature of 135 K; the simple oxide $CrO_2$ [2, 3], extremely useful in magnetic recording; the recently stabilized $BiMnO_3$ perovskite [4, 5] with multiferroic properties, or the complex $\mathrm{CaCu_3Mn_4O_{12}}$ perovskite [6] with colossal magnetoresistance properties. All of them are metastable oxides and revert to a mixture of thermodynamically stable oxides when heated under ambient pressure.

In our group we have been engaged in the preparation and study of metastable oxides containing transition metals in unusual oxidation states, with the help of two complementary high-pressure synthesis procedures: either under a reactive atmosphere of an oxidiz-

ing gas, typically oxygen, or with the application of an external mechanical pressure, which stabilizes the high oxidation states by the compressive effect of the external pressure on the chemical bonds, favoring the smaller ionic sizes corresponding to the high oxidation states.

In this paper we show some results corresponding to two different series of materials prepared under high-pressure conditions: the new family of ferromagnets of stoichiometry $RE\mathrm{FeMnO_5}$, and the series of complex perovskites $RE\mathrm{Cu_3Mn_4O_{12}}$. We describe briefly the antecedents of both families of oxides.

$RE\mathrm{FeMnO_5}$ oxides are derived from the parent family of $RE\mathrm{Mn_2O_5}$ compounds, which were first described in the 1960ies by Bertaut *et al.* [7, 8]. Some $RE\mathrm{Mn_2O_5}$ materials have recently been revisited since they are among the few oxides that show a significant magneto-ferroelectric effect [9, 10] implying a coupling between ferroelectricity and magnetic order in the system: the application of an external magnetic field leads to the appearance of an electrical polarization. The orthorhombic crystal structure of $RE\mathrm{Mn_2O_5}$ (space group *Pbam*) is very interesting since it contains infinite chains of $\mathrm{Mn^{4+}O_6}$ octahedra, linked through $[\mathrm{Mn^{3+}O_5}]$ pyramidal units and bicapped antiprisms $[RE\mathrm{O_8}]$.

$RE\mathrm{Mn_2O_5}$ compounds are antiferromagnets at low temperatures [11], and the magnetic structures, studied from neutron diffraction data, are rather complex and incommensurate with the chemical unit cell. The ordering of the Mn ions is helicoidal and the magnetic moments are aligned in the *ab* plane. Exceptionally, $\mathrm{BiMn_2O_5}$ [12, 13] and $\mathrm{LaMn_2O_5}$ [14] display commensurate magnetic arrangements, defined by the propagation vectors $k = (1/2, 0, 1/2)$ and $k = (0, 0, 1/2)$, respectively.

Aiming to induce new magnetic interactions in the members of the $RE\mathrm{Mn_2O_5}$ family, we recently prepared $RE\mathrm{FeMnO_5}$ oxides, obtained by replacing $\mathrm{Mn^{3+}}$ by $\mathrm{Fe^{3+}}$ in $RE\mathrm{Mn_2O_5}$ ($RE$ = Y, Dy, Ho, Er, Tm, Yb). For instance, whereas $\mathrm{YMn_2O_5}$ is an antiferromagnet with $T_N = 40$ K, $\mathrm{YFeMnO_5}$ is a ferrimagnet below $T_\mathrm{C} \approx 165$ K [15]. The discovery of the new family of ferrimagnets is certainly appealing. These oxides must be prepared under high $\mathrm{O_2}$ pressure, and they have been characterized from the structural point of view from NPD data, complemented with macroscopic magnetic susceptibility and transport measurements.

As to the second topic of this paper, we describe a family of derivatives of the $\mathrm{CaCu_3Mn_4O_{12}}$ oxide, prepared under high-pressure conditions. Among the rare ferromagnetic and half-metallic oxides, the complex perovskite $\mathrm{CaCu_3Mn_4O_{12}}$ [16] is interesting because it exhibits a considerable low-field magnetoresistance at r. t., decoupled at $T_\mathrm{C}$ (355 K) [6]. The crystal structure of $\mathrm{CaCu_3Mn_4O_{12}}$ contains $\mathrm{Cu^{2+}}$ (or other Jahn-Teller transition metal cations, such as $\mathrm{Mn^{3+}}$) at the $A$ positions of the $A\mathrm{BO_3}$ perovskite; this Jahn-Teller cation and $\mathrm{Ca^{2+}}$ are ordered in a 3 : 1 ratio in a $2a_0 \times 2a_0 \times 2a_0$ cubic cell of $Im\overline{3}$ symmetry ($a_0$ = unit cell of the perovskite aristotype). This perovskite is strongly distorted, showing an important tilting of the $\mathrm{MnO_6}$ octahedra, given the small size of the cations at the $A$ positions. Recently, we have been able to synthesize well-crystallized (polycrystalline) samples of some new derivatives of $\mathrm{CaCu_3Mn_4O_{12}}$ at moderate pressures of 2 GPa, starting from very reactive precursors obtained by wet-chemistry procedures, in the presence of $\mathrm{KClO_4}$ as an oxidizing agent [17]. In this system, $\mathrm{Ca^{2+}}$ cations can be replaced by rare earths in the $RE\mathrm{Cu_3Mn_4O_{12}}$ ($RE$ = rare earths) family, implying an electron doping effect that affects the magnetic and transport properties, as demonstrated for $RE$ = La, Ce, Nd and also for Th [18,19]. With the aim of studying the structural, magnetic and magnetotransport properties of this promising system, we have prepared new $RE\mathrm{Cu_3Mn_4O_{12}}$ compounds with $RE$ = Pr, Sm, Eu, Gd, Tb, Dy, Ho, Tm, Yb. These materials have been fully characterized by neutron powder diffraction (NPD) and X-ray diffraction (XRD), magnetic and magnetotransport measurements.

## Experimental Section

$RE\mathrm{FeMnO_5}$ compounds ($RE$ = Y, Tb, Dy, Ho, Er, Tm, Yb) were prepared in polycrystalline form from citrate precursors obtained by a wet-chemistry procedure. Stoichiometric amounts of analytical grade $RE_2\mathrm{O_3}$, $\mathrm{FeC_2O_4 \cdot 2H_2O}$ and $\mathrm{MnCO_3}$ were dissolved in citric acid; the solution was slowly evaporated, leading to a resin which was dried at 120 °C and slowly decomposed at temperatures up to 600 °C in air. High oxygen pressure treatments were performed in a VAS furnace. About 2 g of the precursor powder were contained in a gold can during the oxygenation process. The sample was slowly heated to 900 °C at a final pressure of 200 bar, and held at this temperature for 12 h. The product was finally cooled, under pressure, at 300 °C $\mathrm{h^{-1}}$ to r. t. Finally, the oxygen pressure was slowly released.

The synthesis of $RE\mathrm{Cu_3Mn_4O_{12}}$ compounds also required the preparation of very reactive precursors obtained by wet-chemistry techniques. A mixture of $\mathrm{Cu(NO_3)_2 \cdot 3H_2O}$,

$MnCO_3$ and the corresponding $RE_2O_3$ oxide was dissolved in citric acid; the solution was slowly evaporated and the resulting resin was decomposed at temperatures up to 800 °C. These precursors were thoroughly ground with $KClO_4$ (30% in weight), put into a gold capsule (8 mm dia., 10 mm length), which was sealed and placed in a cylindrical graphite heater. The reactions were carried out in a piston-cylinder press (Rockland Research Co.) at a pressure of 2 GPa at 1000 °C for 60 min. The ground product was washed with a dilute aqueous solution of $HNO_3$, in order to dissolve KCl and any unreacted phase produced in the decomposition of $KClO_4$.

All products were initially characterized by laboratory XRD (Cu$K_\alpha$, $\lambda = 1.5406$ Å) for phase identification and phase purity. For the structure refinements, NPD data were collected at r. t. at the high resolution D2B neutron diffractometer of ILL-Grenoble and at the HRPT diffractometer of the SINQ spallation source at the PSI, Zürich. Both crystallographic and magnetic structures were refined from NPD data by Rietveld methods, using the refinement program FULL PROF. The *dc* magnetic susceptibility was measured with a commercial SQUID magnetometer on powdered samples, in the temperature range of 2 to 400 K under magnetic fields up to 16 T.

## Results

### *The REFeMnO$_5$ series*

*RE*FeMnO$_5$ oxides were obtained as dark brown polycrystalline powders. The preparation from the precursor powders required the presence of moderate $O_2$ pressures in order to partially oxidize Mn to the tetravalent oxidation state. The XRD patterns could be indexed in an orthorhombic unit cell, isotypic to *RE*$Mn_2O_5$, with no additional peaks which could indicate the presence of superstructures or a departure of the mentioned symmetry.

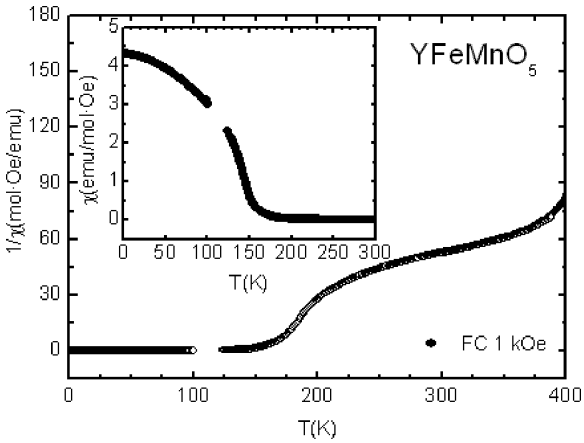


Fig. 1. Thermal evolution of the magnetic susceptibility of YFeMnO$_5$.

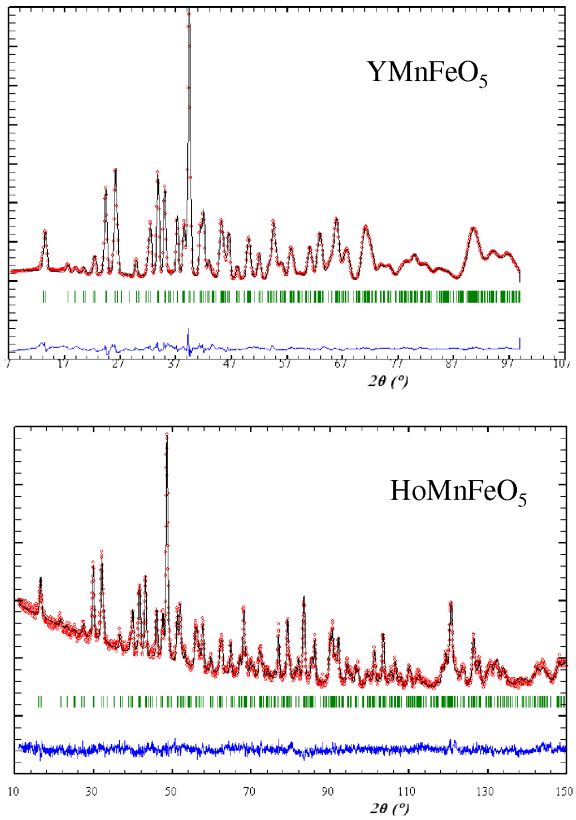


Fig. 2. Rietveld-refined NPD patterns for *RE*FeMnO$_5$ (*RE* = Y, Ho) at r. t.

The thermal variation of the *dc* susceptibility is shown in Fig. 1. As it can be seen in the inset of Fig. 1, the susceptibility undergoes a remarkable increase below 165 K, revealing the onset of a magnetic transition at $T_C \approx 165$ K. Microscopic neutron diffraction measurements described below demonstrate that the anomaly at $T_C = 165$ K indeed corresponds to the onset of a long-range ferrimagnetic structure.

The crystallographic structure was refined from high resolution NPD data collected at r. t. with $\lambda = 1.594$ Å in the space group *Pbam*. Fe atoms occupy the 4*h* (*x*, *y*, 1/2) site (pyramidal positions), whereas the Mn atoms are located at the 4*f* (0, 1/2, *z*) site (octahedral positions). The experimental and calculated NPD patterns for two selected samples, YFeMnO$_5$ and HoFeMnO$_5$, are compared in Fig. 2. A view of the crystal structure along the *c* axis is presented in Fig. 3. The $Mn^{4+}O_6$ octahedra form infinite chains along the *c* direction linked *via* the equatorial oxygen atoms O2 and O3. In

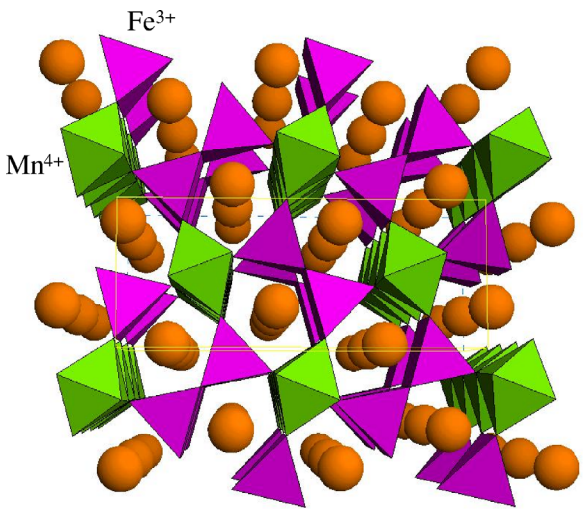


Fig. 3. A view of the crystallographic structure of $RE$FeMnO$_5$ oxides, approximately along the $c$-axis. Octahedra and square pyramids correspond to (Mn)$^{4+}$O$_6$ and (Fe)$^{3+}$O$_5$ polyhedra. Spheres represent the $RE$ atoms.

the Fe$^{3+}$O$_5$ pyramids the O3 oxygen atom is in the axial position, whereas the O1 and O4 oxygen atoms are in the base plane. Pairs of Fe$^{3+}$O$_5$ pyramids, doubly linked by O1 oxygen atoms, form a dimeric unit Fe$_2$O$_{10}$. Four chains of Mn$^{4+}$O$_6$ octahedra are linked by a dimeric unit through the O3 and O4 oxygen atoms.

The unit cell parameter variations along the series of stable oxides, from TbFeMnO$_5$ to TmFeMnO$_5$, are presented in Fig. 4. There is a monotonous unit cell variation due to the lanthanoid contraction, excepting Y, which seems to exhibit a larger ionic radius than tabulated. It is worth commenting that single-phase oxides $RE$FeMnO$_5$ are only stabilized for medium-sized rare earths Tb, Dy, Ho, Er, Tm, Y. The hypothetical end of the series, LaFeMnO$_5$, is not stable; for $RE$ = Nd$\cdots$Gd, competitive $RE$MnO$_3$ and $RE$FeO$_3$ perovskites are present as secondary phases; for $RE$ = Yb, Lu, hexagonal $RE$MnO$_3$ oxides are formed.

In $RE$Mn$_2$O$_5$, the Mn$^{4+}$O$_6$ octahedra are fairly flattened [1, 2], with two bonds significantly shorter than the remaining four bonds, *e. g.* Mn1–O3 of 1.858(5) Å as illustrated in Fig. 5 for ErFeMnO$_5$. The average Mn–O distance is 1.898 Å. This is also observed in ErFeMnO$_5$, with Mn1–O3 of 1.820 Å and an average value of 1.891 Å. Regarding the square pyramids, the Fe$^{3+}$O$_5$ units are flattened, as the axial Fe-O3 bond length is the shortest one (1.898(5) Å), which is in contrast with $RE$Mn$_2$O$_5$, where the Mn2-O3 bond in

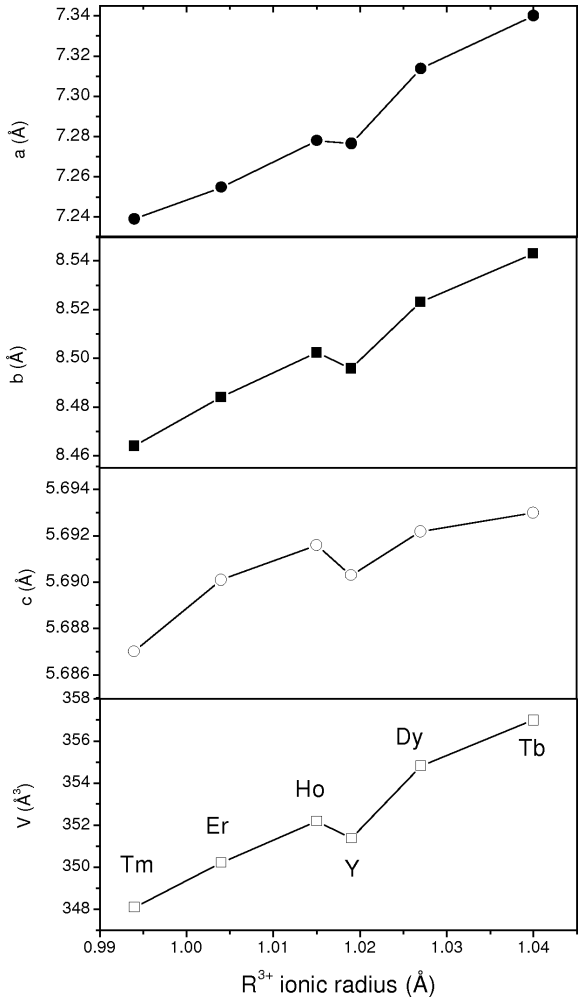


Fig. 4. Unit cell parameter variations with the ionic size of $RE^{3+}$ in $RE$FeMnO$_5$.

the axial position is the longest one in the Mn$^{3+}$O$_5$ pyramids (2.023(6) Å). This is probably related to the Jahn-Teller character of the Mn$^{3+}$ cations, favoring an increase of the axial bond lengths, in contrast with the non-Jahn-Teller character of Fe$^{3+}$ ($3d^5$ configuration).

The temperature-dependent NPD patterns show that there is some magnetic contribution on the low-angle reflections below the characteristic Curie temperatures. As the magnetic peaks appear at the crystallographic Bragg positions, the size of the magnetic unit cell coincides with the chemical one, and therefore the magnetic structure can be defined with a propagation vector $k = 0$. The possible magnetic structures compatible with the orthorhombic crystallographic structure, space group *Pbam*, and associated with the propaga-

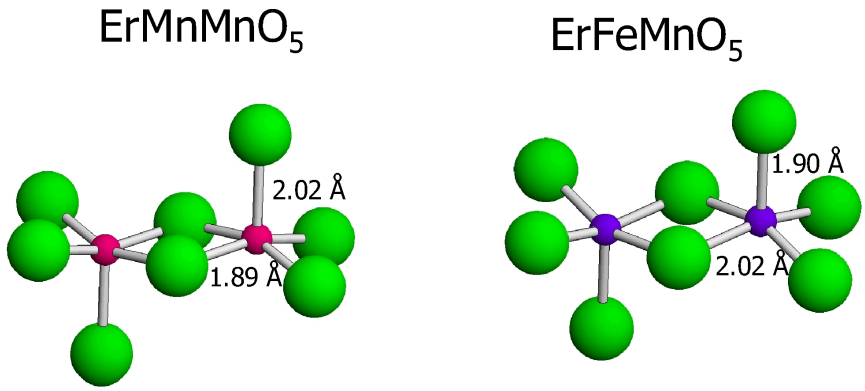


Fig. 5. Dimeric units $Mn_2O_{10}$ and $Fe_2O_{10}$ in $ErMn_2O_5$ and $ErFeMnO_5$, respectively.

tion vector $k = 0$, were determined by considering the representation analysis technique of the group theory described by Bertaut [20]. For the Mn and Fe atoms in the $4f$ and $4h$ sites, respectively, the basis vectors have been taken from Ref. [15].

Upon comparing the different solutions, the best agreement with the experimental data is obtained if only the Mn and Fe atoms are antiferromagnetically ordered; the corresponding spin arrangement for the Mn and Fe atoms is given by the basis vectors (0, 0, $F_z$) and (0, 0, $F_z'$), respectively. This implies a global ferrimagnetic structure.

A view of the magnetic structure is displayed in the upper panel of Fig. 6. The magnetic moments for both Mn and Fe atoms are oriented along the $c$ direction. The goodness of the fit, including the magnetic structure, is shown in the lower panel of Fig. 6. The presence of $Fe^{3+}$ cations is not only responsible for the different strength of the magnetic coupling with respect to the $RE\,Mn_2O_5$ parent compounds, but also for the sign of some of the superexchange interactions. Therefore, it is worthwhile considering the magnetic interactions that are driving the long-range magnetic order. It seems reasonable to think that the strong superexchange Fe–O1–Fe interactions within the $Fe_2O_{10}$ units trigger the onset of the magnetic ordering of the $Fe^{3+}$ spins above $T_C$. Given the Fe–O1–Fe angles close to 90° within the dimeric units, these interactions are ferromagnetic in origin, according to the Goodenough-Kanamori rules [21, 22]. It is plausible that the $Fe^{3+}$ spins in the dimeric units are coupled (but not long-range ordered) above $T_C$. Immediately below $T_C$, the appearance of strong antiferromagnetic interactions between $Fe^{3+}$ of the dimeric units and $Mn^{4+}$ of the chains *via* O4 oxygen atoms would give rise to the long-range ordering, accounting for the appearance of magnetic scattering at the low-angle reflections.

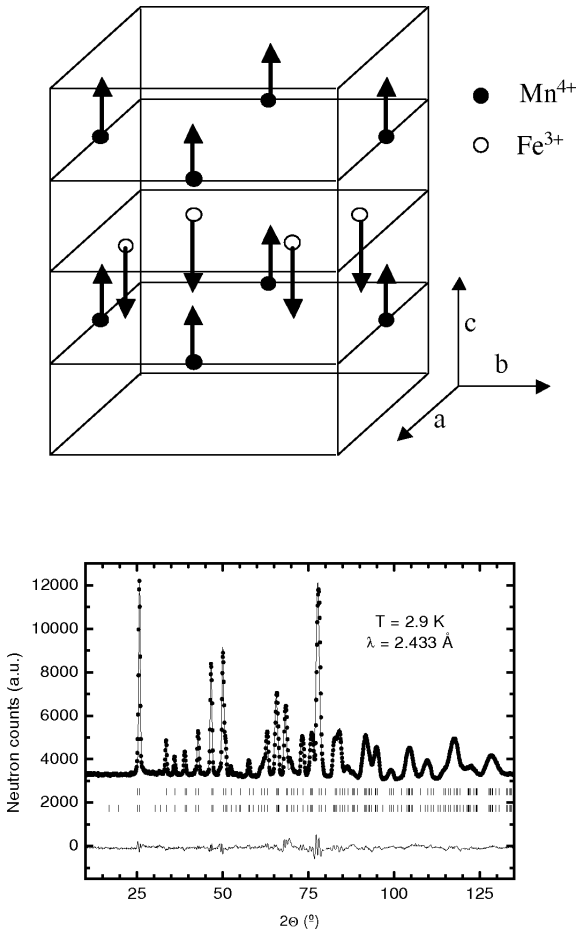


Fig. 6. Magnetic structure for $RE\,FeMnO_5$ (upper panel). Observed (crosses), calculated (solid line) and difference (bottom line) NPD patterns for $YFeMnO_5$ at $T = 1.5$ K. The second series of Bragg positions corresponds to the magnetic structure.

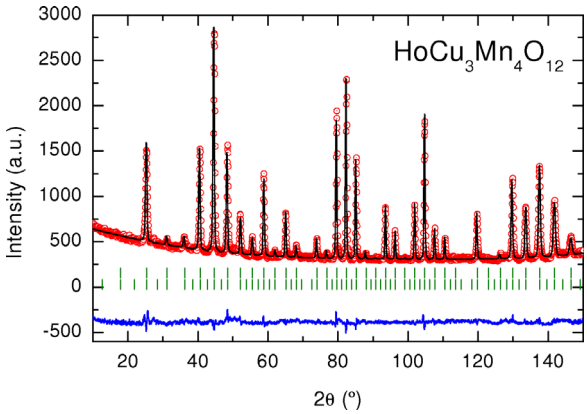


Fig. 7. Observed (circles), calculated (full line), and difference (bottom) NPD Rietveld profiles for $HoCu_3Mn_4O_{12}$ at r. t. The second series of Bragg reflections corresponds to the magnetic structure.

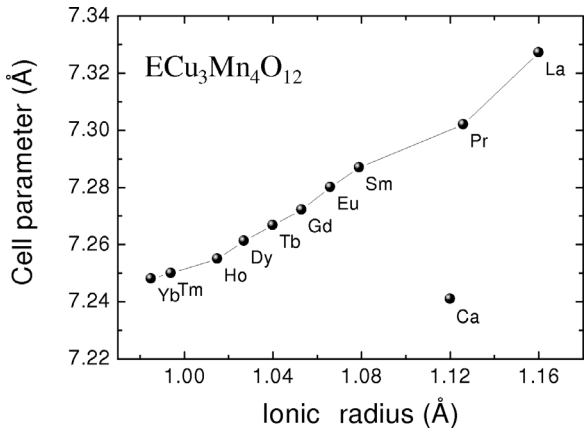


Fig. 8. Unit cell parameter evolution with the ionic radius of the rare earth cation. The parameter of $CaCu_3Mn_4O_{12}$ is given for comparison: the ionic radii of eight-fold coordinated cations are considered in all cases.

*The $RECu_3Mn_4O_{12}$ series*

The materials with non-absorbing rare earths have also been studied by NPD at r. t., allowing us to determine the subtle structural features which are related to the observed physical properties. The structural refinement from NPD patterns was performed in the space group $Im\bar{3}$ (No. 204), with rare earth atoms at 2*a* (0, 0, 0) positions (*A′* site), Cu at 6*b* (0, 1/2, 1/2; *A* site), Mn at 8*c* (1/4, 1/4, 1/4; *B* site) and O at 24*g* (0, *y*, *z*) sites. As the materials are ferrimagnetically ordered at r. t., the magnetic structure was included as a second phase in the final refinement, by considering Mn and Cu substructures antiferromagnetically coupled. Fig. 7 shows an excellent agreement between the observed and calculated NPD profiles at r. t. for $HoCu_3Mn_4O_{12}$ ($R_I \approx$ 8%). Similar fits have been obtained for all the samples. The subsequent refinement of the oxygen content gave no significant deviation from the full stoichiometry.

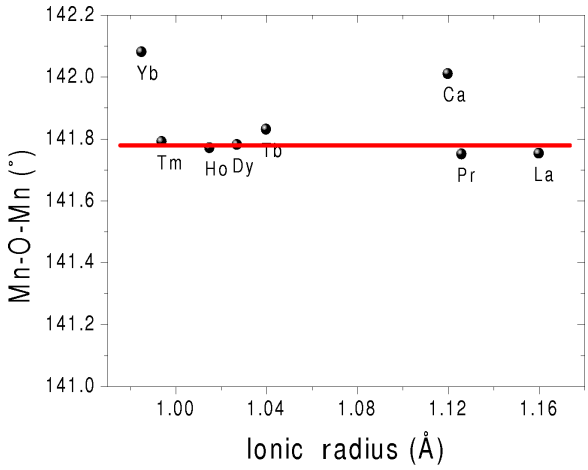


Fig. 9. Variation of the Mn–O–Mn angle across the $RECu_3Mn_4O_{12}$ series.

Fig. 8 shows the unit cell parameter *a* as a function of the ionic radii of the rare earth elements in eight-fold coordination. Notice that the size of the cell is, in all cases, significantly larger than that of the undoped $Ca^{2+}$ compound, which suggests that the main driving force for the unit cell expansion is the electronic injection effect on bands of Mn–O origin. In fact, Mn–O distances are considerably longer than those observed in $CaCu_3Mn_4O_{12}$, of 1.911 Å. As shown in Fig. 9, it is surprising that the Mn–O–Mn angle is quite insensitive to the size of the $RE^{3+}$ cation (unlike it happens in other *RE* containing perovskite series, such as $RENiO_3$), since the tilting of the $MnO_6$ octahedra is mainly determined by the presence of three $Cu^{2+}$ cations *versus* a single $RE^{3+}$ cation at the *A′* positions.

Fig. 10 shows the steep increase of magnetization with decreasing temperature characteristic of a spontaneous ferromagnetic ordering for all the samples. For all *RE* substituted samples, the inflexion point in the magnetization indicating the ferromagnetic Curie temperature ($T_C$) increases remarkably up to almost 400 K, well above the reported Curie temperature of the parent compound $CaCu_3Mn_4O_{12}$ ($T_C = 355$ K) or $CaCu_{2.5}Mn_{4.5}O_{12}$ ($T_C = 345$ K).

The study of the magnetic structures has demonstrated that Mn and Cu spins are coupled antiferro-

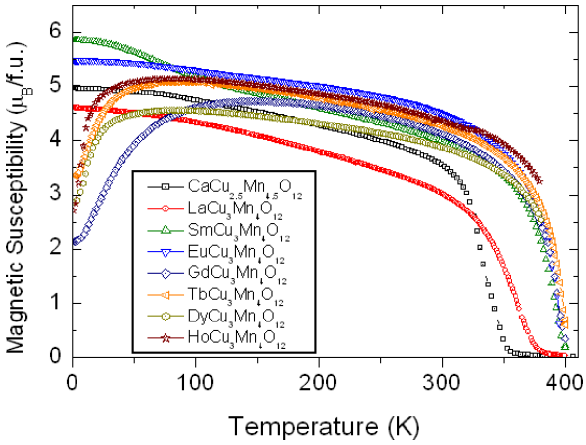


Fig. 10. Temperature dependence of the *dc* magnetic susceptibility for $RECu_3Mn_4O_{12}$ compounds.

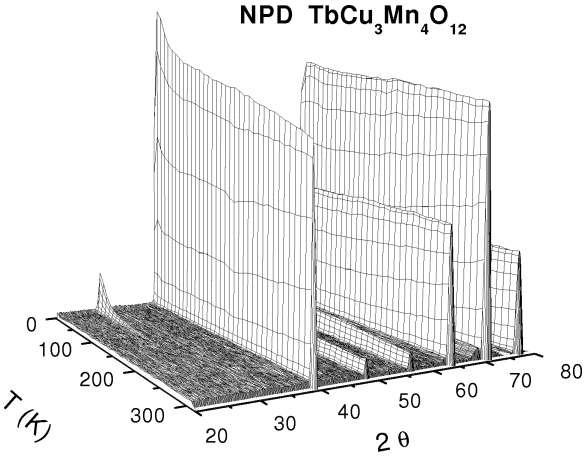


Fig. 11. Thermal evolution of the NPD patterns for $TbCu_3Mn_4O_{12}$.

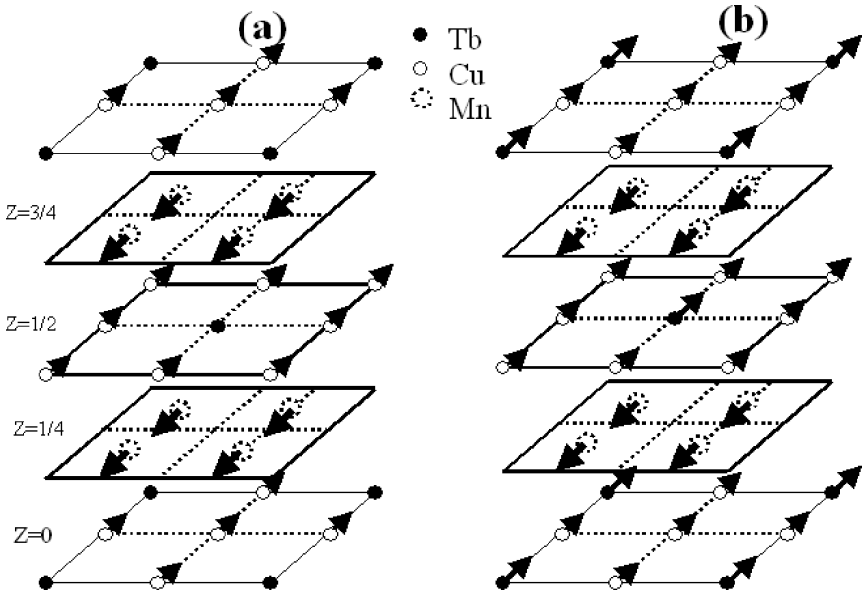


Fig. 12. Magnetic structure of $TbCu_3Mn_4O_{12}$ (a) above 80 K and (b) below 80 K.

magnetically. At low temperatures (< 100 K), the rare earth moment plays an important role in the total magnetization, as *e. g.* in the Pr, Gd, Tb, Dy and Ho perovskites. The rare earth moment seems to become antiferromagnetically coupled with the Mn substructure, and therefore the magnetization undergoes an important decrease (Fig. 11). This has been experimentally shown from the thermal evolution of the sequential NPD collected between 2 K and r. t.: an example is illustrated in Fig. 11 for $TbCu_3Mn_4O_{12}$.

The low angle NPD reflections progressively increase as a consequence of the ferrimagnetic coupling of Mn and Cu magnetic moments below $T_C$; a second anomaly is observed in the appearance of an extra reflection below 80 K which is a consequence of the long-range magnetic ordering of $Tb^{3+}$ moments. A good fit to the NPD data is achieved with the magnetic structure model shown in Fig. 12, above and below 80 K. Below this temperature, Tb moments become ferromagnetically ordered to $Cu^{2+}$ spins and antiparallel to the $Mn^{4+}$ moments.

## Conclusions

High-pressure techniques are a powerful tool for the stabilization of metastable oxides. Working un-

der moderate $O_2$ pressure (200 bar), we have been able to prepare a new series of ferrimagnetic oxides, obtained by replacing $Mn^{3+}$ by $Fe^{3+}$ in the parent $RE\mathrm{Mn_2O_5}$ compounds. The crystal and magnetic structures have been studied by NPD, revealing the onset of a ferrimagnetic structure below $T_C \approx 165$ K, characterized by the propagation vector $k = 0$. Some new ferrimagnets with $RE\mathrm{Cu_3Mn_4O_{12}}$ stoichiometry have been prepared at moderate pressures of 2 GPa by replacing $Ca^{2+}$ by $RE^{3+}$ rare earth cations; the concomitant electronic injection leads to a substantial increase of $T_C$. The crystal and magnetic structures of the new materials, studied from NPD data, show a ferrimagnetic coupling between $Mn^{3+/4+}$ and $Cu^{2+}$ spins; at lower temperatures the rare earth magnetic moment participates in the magnetic structure, exhibiting an antiferromagnetic coupling with the Mn substructure.


[1] E. V. Antipov, S. M. Loureiro, C. Chaillout, J. J. Capponi, P. Bordet, J. L. Tholence, S. N. Putilin, M. Marezio, Phys. C **215**, 1 (1993).

[2] K. P. Kamper, W. Schmitt, G. Guntherodt, R. J. Gambino, R. Ruf, Phys. Rev. Lett. **59**, 2788 (1987).

[3] L. Ranno, A. Barry, J. M. D. Coey, J. Appl. Phys. **81**, 5774 (1997).

[4] T. Atou, H. Chiva, K. Ohoyama, Y. Yamaguchi, Y. Syono, J. Solid State Chem. **145**, 639 (1999).

[5] K. M. Robe, N. Hill, Phys. Rev. B **59**, 8759 (1999).

[6] Z. Zeng, M. Greenblatt, M. A. Subramanian, M. Croft, Phys. Rev. Lett. **82**, 3164 (1999).

[7] S. Quezel-Ambrunaz, E. F. Bertaut, G. Buisson, C. R. Acad. Sci. **258**, 3025 (1964).

[8] E. F. Bertaut, G. Buisson, A. Durif, A. Mareschal, M. C. Montmory, S. Quezel-Ambrunaz, Bull. Soc. Chim. Fr. 1132 (1965).

[9] A. Kadomtseva, Y. F. Popov, G. P. Vorobev, K. I. Kamilov, P. N. Makhov, M. M. Tehranchi, A. Phirouznia, Physica B: Condensed Matter **329 – 333**, 856 (2003).

[10] Y. F. Popov, A. M. Kadomtseva, S. S. Krotov, G. P. Vorob'ev, M. M. Lukina, Ferroelectrics **279**, 147 (2002).

[11] J. A. Alonso, M. T. Casais, M. J. Martínez-Lope, J. L. Martínez, M. T. Fernández-Díaz. J. Phys.: Condens. Matter **9**, 8515 (1997).

[12] A. Muñoz, M. T. Casais, M. J. Martínez-Lope, J. L. Martínez, J. A. Alonso, M. T. Fernández-Díaz, Phys. Rev. B **65**, 144423 (2002).

[13] E. F. Bertaut, G. Buisson, S. Quezel-Ambrunaz, G. Quezel, Solid State Commun. **5**, 25 (1967).

[14] A. Muñoz, J. A. Alonso, M. T. Casais, M. J. Martínez-Lope, J. L. Martínez, M. T. Fernández-Díaz, Eur. J. Inorg. Chem. 685 (2005).

[15] A. Muñoz, J. A. Alonso, M. J. Martínez-Lope, J. L. Martínez, Chem. Mater. **35**, 101021 (2004).

[16] J. Chenavas, J. C. Joubert, M. Marezio, B. Bochu, J. Solid State Chem. **14**, 25 (1975).

[17] J. Sánchez-Benítez, J. A. Alonso, M. J. Martínez-Lope, M. T. Casais, J. L. Martínez, A. de Andrés, M. T. Fernández-Díaz, Chem. Mater. **15**, 2193 (2003).

[18] J. A. Alonso, J. Sánchez-Benítez, A. De Andrés, M. J. Martínez-Lope, M. T. Casais, J. L. Martínez, Appl. Phys. Lett. **83**, 2623 (2003).

[19] J. Sánchez-Benítez, J. A. Alonso, A. De Andrés, M. J. Martínez-Lope, M. T. Casais, J. L. Martínez, J. Magn. Magn. Mater. **272** E1407 (2004).

[20] E. F. Bertaut, in G. T. Rado, H. Shul, (eds): Magnetism, Vol. III, Chapter 4, Academic Press, New York (1963).

[21] J. B. Goodenough, Phys. Rev. **100**, 564 (1955).

[22] J. Kanamori, J. Phys. Chem. Solids **10**, 87 (1959).